

Post myocardial infarction of the left ventricle: the course ahead seen by cardiac MRI

Pier Giorgio Masci¹, Jan Bogaert²

¹Magnetic Resonance Imaging and Cardiovascular Medicine Departments, Fondazione CNR/Regione Toscana 'G. Monasterio', Pisa, Italy; ²Radiology Department, Medical Imaging Research Center, University Hospitals Leuven, Herestraat 49, B-3000 Leuven, Belgium

Corresponding to: Jan Bogaert, MD, PhD. Radiology - Medical Imaging Research Center, Herestraat 49, B-3000 Leuven-Belgium. Tel: +3216340485; fax: +3216343765. Email: jan.bogaert@uz.kuleuven.ac.be.

Abstract: In the last decades, cardiac magnetic resonance imaging (MRI) has gained acceptance in cardiology community as an accurate and reproducible diagnostic imaging modality in patients with ischemic heart disease (IHD). In particular, in patients with acute myocardial infarction (MI) cardiac MRI study allows a comprehensive assessment of the pattern of ischemic injury in term of reversible and irreversible damage, myocardial hemorrhage and microvascular obstruction (MVO). Myocardial salvage index, derived by quantification of myocardium (area) at risk and infarction, has become a promising surrogate end-point increasingly used in clinical trials testing novel or adjunctive reperfusion strategies. Early post-infarction, the accurate and reproducible quantification of myocardial necrosis, along with the characterization of ischemic myocardial damage in its diverse components, provides important information to predict post-infarction left ventricular (LV) remodeling, being useful for patients stratification and management. Considering its non-invasive nature, cardiac MRI suits well for investigating the time course of infarct healing and the changes occurring in peri-infarcted (adjacent) and remote myocardium, which ultimately promote the geometrical, morphological and functional abnormalities of the entire left ventricle (global LV remodeling). The current review will focus on the cardiac MRI utility for a comprehensive evaluation of patients with acute and chronic IHD with particular regard to post-infarction remodeling.

Key Words: Magnetic resonance imaging (MRI); ischemic heart disease (IHD); left ventricular (LV); myocardial viability



Submitted Apr 09, 2012. Accepted for publication Apr 26, 2012.

doi: 10.3978/j.issn.2223-3652.2012.04.06

Scan to your mobile device or view this article at: <http://www.thecdt.org/article/view/682/751>

Introduction

Over the past decades cardiac magnetic resonance imaging (MRI) has emerged as an accurate diagnostic technique for the evaluation of patients with ischemic heart disease (IHD). In the acute setting of IHD, i.e. acute myocardial infarction (MI), comprehensive cardiac MRI study enables to precisely characterize the ischemic myocardial injury by differentiating the reversible from irreversible damaged tissue along with the depiction of microvascular injury. In the post-infarction phase, regional and global left ventricular (LV) post-infarction remodeling along with viability assessment by cardiac MRI provide crucial information for patients management and risk stratification.

Cardiac MRI in acute IHD - exploring the jeopardized myocardium

The study of acute ischemic myocardial damage has to consider the complexity of events occurring in the evolving MI. An acute infarct goes through a series of inflammatory and healing stages with replacement of the dead myocardium by collagenized scar tissue (1). This process aims to minimize the detrimental consequences due to the loss of function of the necrotic myocardium, initiating and perpetuating a series of geometrical, mechanical and neuro-hormonal changes which may ultimately lead to LV dysfunction and heart failure. Comprehensive cardiac MRI study is ideal for an accurate *in-vivo* depiction of the pathophysiological

phenomena occurring acutely in the infarcted myocardium using its array of techniques.

Characterization of myocardium (area) at risk

In the last years, growing evidences have been cumulated on the value of T2-weighted short-tau inversion-recovery (STIR) imaging for the detection of the myocardium (or area) at risk (2), i.e. the ischemic myocardium at the moment of coronary occlusion which can be potentially salvaged by reperfusion. Indeed, T2-weighted STIR is particularly sensitive to the increase of tissue free water (infarct-related edema) which constantly accompanies ischemic myocardial damage irrespective of concomitant necrosis (3,4). Myocardial edema (ischemia causes dysfunction of ATP-dependent sodium-potassium channels, altering trans-membrane sodium gradients causing intracellular edema) is an early feature in ischemic damage and T2-weighted imaging may serve as a very useful diagnostic marker in patients with unstable angina or evolving myocardial infarction in the emergency department (5,6). In particular on T2-weighted STIR imaging the myocardial edema appears as an hyperintense (bright) region (*Figure 1*). Abdel-Aty *et al.* (7) recently showed that edema imaging depicts acute ischemic injury within the first 30 minutes after onset of ischemia, before the onset of irreversible myocardial injury as detected by troponin elevation and occurrence of late gadolinium enhancement (LGE). Experimentally Aletras *et al.* (2) demonstrated that edematous region on T2-weighted STIR imaging two days after a reperfused infarction corresponded to the area at risk depicted by microsphere injection at the time of coronary occlusion (i.e. the reference standard). Additionally, the extent of myocardium at risk was significantly larger than the infarcted myocardium, indicating that edematous region visualized by T2-weighted STIR imaging comprised both reversible and irreversible damaged myocardium (i.e. jeopardized myocardium). This technique has been recently tested against single-photon emission computed tomography (SPECT) in patients with reperfused ST-segment elevation MI. In particular, the perfusion defect visualized by ^{99m}Tc-tetrofosmin SPECT before primary percutaneous coronary intervention (PCI) mirrored myocardial edema detected by T2-weighted STIR imaging 7 days after the acute event (8). Accordingly, T2-weighted STIR imaging allows an accurate retrospective and ionizing-free determination of the myocardium (area) at risk without interfering with patients management in the

acute phase. Additionally, in patients with acutely reperfused MI we and other groups validated this technique against the angiographic score of myocardium at risk (9,10). Recently skepticism has been recently raised about the accuracy of T2-weighted STIR imaging in depicting myocardium (area) at risk due to its inherent sensitivity to artifacts and poor reproducibility (11). Additionally this sequence suffers of inherently low signal-to-noise ratio and is prone to 'slow flow' artifact at boundary between endocardium and ventricular cavity. It is important to recognize that most of our knowledge on the determination of area at risk by T2-weighted STIR imaging derives from relative small experimental studies and further studies are warranted. In this context, promising sequences come out such as T2-prepared steady state free precession or T2-mapping (12,13). Of note, T2-weighted abnormalities are most evident in the acute and sub-acute phase post-infarction and slowly fade away because of resorption of infarct-related myocardial edema and inflammation (8). Thus, this sequence allows to differentiate between an acute or chronic MI (14) since the former is accompanied by myocardial edema whereas in chronic MI no edema is visualized on T2-weighted STIR imaging. Finally, T2-weighted imaging enables to depict post-reperfusion myocardial hemorrhage. Indeed, differently from non-reperfused infarcts, which are typically devoid of hemorrhage, reperfused infarcts are frequently associated with significant interstitial extravasation of red blood cells due to severe microvascular damage as a consequence of ischemia-reperfusion injury (15). *In-vivo* and autopsy studies have shown the potential of T2-weighted imaging in the depiction of intramyocardial hemorrhage by exploiting the paramagnetic properties of hemoglobin breakdown products, which shortens consistently T2-relaxation time (16,17). Thus, on edema imaging hemorrhagic infarcts will have heterogeneous appearance typically presenting with a hypo-intense core and a peripheral hyperintense rim, and can easily be differentiated from non-hemorrhagic infarcts which appear as homogeneously hyperintense myocardium (*Figure 2*). In a study of 98 patients with reperfused ST-segment myocardial infarction, we found intramyocardial hemorrhage in 25% of patients (18). Patients with hemorrhagic infarcts had greater infarct size and infarct transmural, larger no-reflow zone and less myocardial salvage. Intramyocardial hemorrhage was an independent predictor of adverse LV remodeling irrespective of the initial infarct size. Afterward Eitel *et al.* (19) showed that T2-weighted myocardial hemorrhage was an independent predictor of major adverse cardiovascular

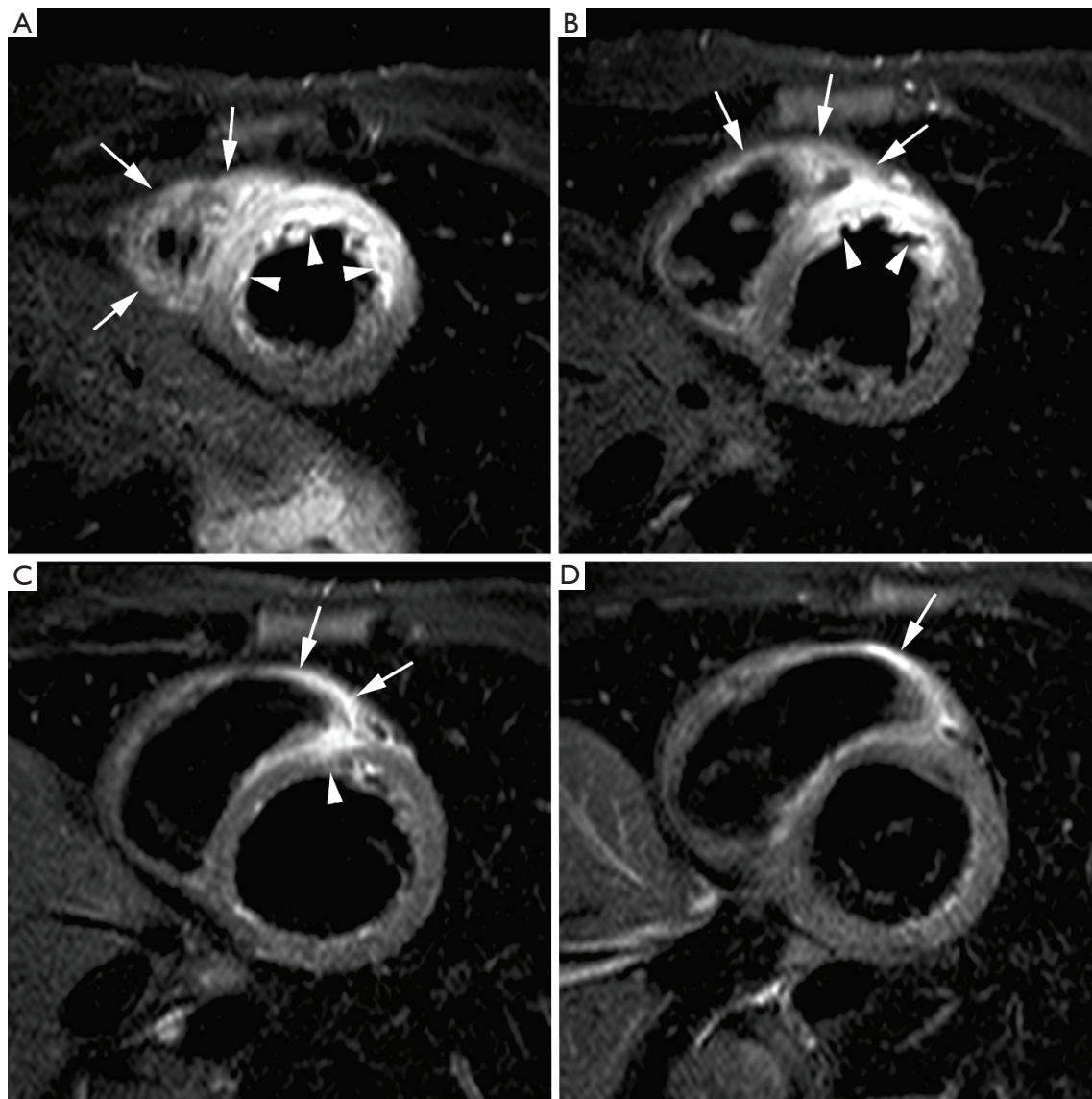


Figure 1 Edema imaging in a patient with a reperfused acute anteroseptal myocardial infarction (day 3 post MI). Short-axis T2-weighted STIR imaging at 4 levels (A-D). The jeopardized, edematous myocardium is visible as the myocardium showing increased signal intensity (*arrowheads*, A-C). Note the extension of the edema towards the adjacent RV anterior wall (*arrows*, A-D). Adapted from *Ischemic Heart Disease* by Bogaert J and Dymarkowski S, in *Clinical Cardiac MRI Second Edition*, Bogaert J, Dymarkowski S, Taylor AM, Muthurangu V (eds). Springer Heidelberg, Germany (ISBN 978-3-642-23034-9)

events at 6 months after MI.

Characterization of myocardial infarction in the acute phase

Contrast-enhanced cardiac MRI with late gadolinium enhancement (LGE) technique is an accurate modality to visualize and quantify irreversible ischemic damage in the context of myocardium at risk (20). This consists in

performing T1-weighted inversion-recovery segmented gradient echo sequence between 10 and 20 minutes after a bolus of gadolinium-based contrast agent (CA). Although the mechanisms of LGE have yet to be fully elucidated, however, it has been ascertained that the time-varying enhancement is broadly different in the infarcted and normal myocardium. In the infarcted myocardium the wash-in and wash-out phases of CA are consistently delayed as compared to the

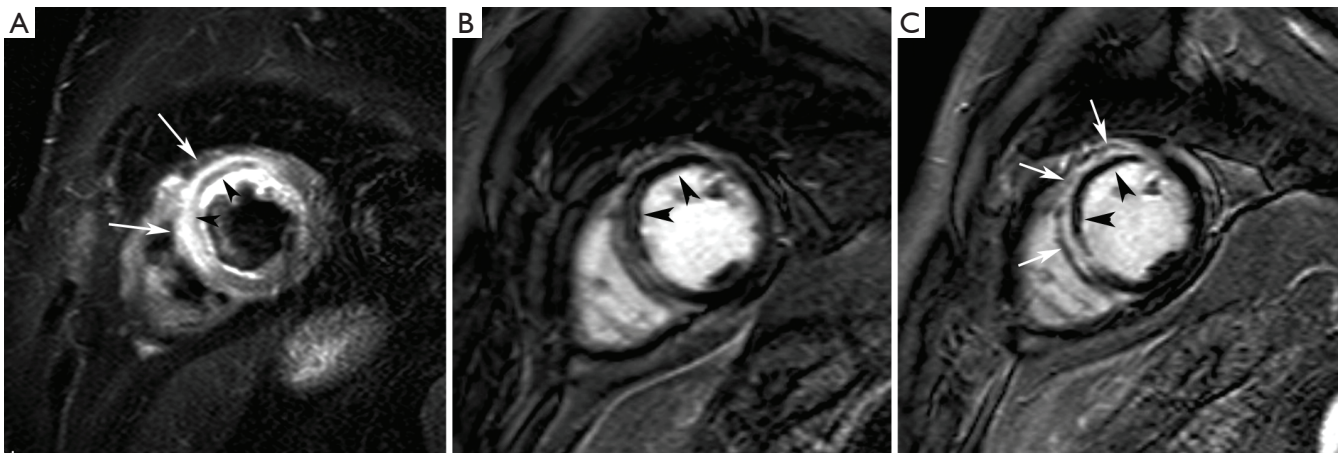


Figure 2 Hemorrhagic myocardial infarction. Short-axis T2-weighted STIR imaging (A), early gadolinium imaging (B) and late gadolinium imaging (C) in a patient with an extensive reperfused acute anteroseptal myocardial infarction. Presence of an extensive zone of myocardial edema in the LV anteroseptal wall (*arrows*, A) with evidence of concomitant myocardial hemorrhage (*arrowheads*, A). On early gadolinium imaging, a large zone of microvascular obstruction is present (*arrowheads*, B). At late imaging, a significant shrinkage of the microvascular obstruction has occurred (*arrowheads*, C) while the infarct has substantially become enhanced (*arrows*, C). Adapted from *Ischemic Heart Disease* by Bogaert J and Dymarkowski S, in *Clinical Cardiac MRI Second Edition*, Bogaert J, Dymarkowski S, Taylor AM, Muthurangu V (eds). Springer Heidelberg, Germany (ISBN 978-3-642-23034-9)

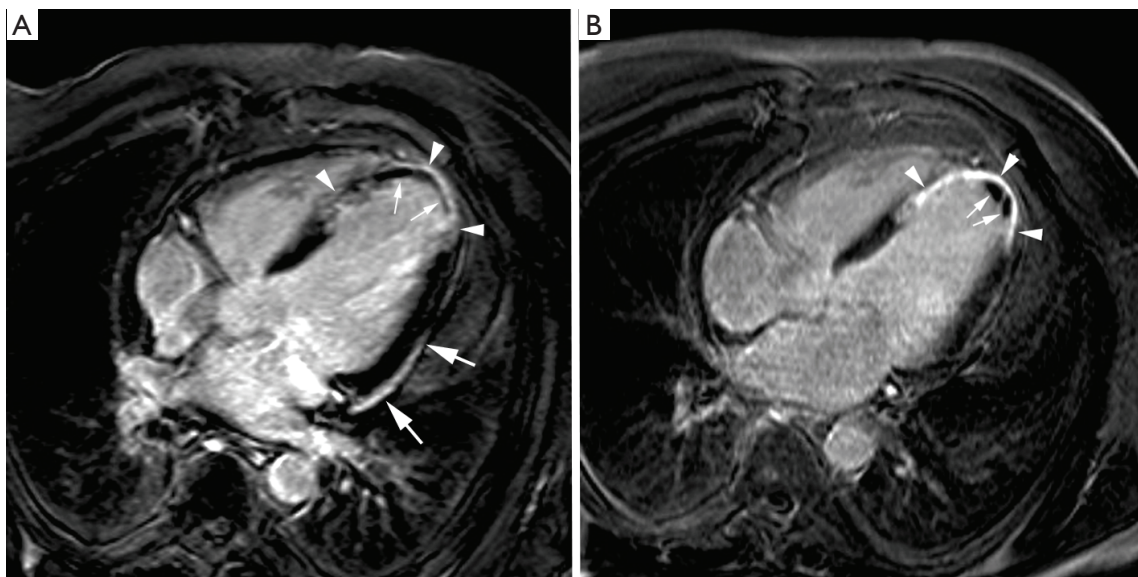


Figure 3 Evolution of an acute towards a healed myocardial infarction in a 52-year-old patient with anteroapical infarction. Late gadolinium imaging in horizontal image plane at 1 week (A) and 4 months (B) after the acute event. At 1 week, presence of diffuse enhancement of the apical part of the ventricular septum and LV apex (*arrowheads*, A) with large area of microvascular obstruction (*small arrows*, A). Note the presence of some pericardial enhancement over the laterobasal part of the LV (*arrows*, A). At 4 month follow-up, the infarct has thinned and strongly enhances (*arrowheads*, B). Note the presence of a small mural thrombus in LV apex (*arrows*, B). Adapted from *Ischemic Heart Disease* by Bogaert J and Dymarkowski S, in *Clinical Cardiac MRI Second Edition*, Bogaert J, Dymarkowski S, Taylor AM, Muthurangu V (eds). Springer Heidelberg, Germany (ISBN 978-3-642-23034-9)

normal myocardium, so that on late post-contrast imaging CA concentration is higher in the infarcted myocardium. Using the inversion-recovery technique, the signal intensity of non-infarcted myocardium is artificially nulled so

that it appears hypointense (dark), whereas the infarcted myocardium appears hyperintense (bright) yielding a high contrast to noise ratio (*Figure 3*). Several patho-physiological factors have been implicated in the 'late' accumulation of

CA in the infarcted tissue, even though the increase of distribution volume is likely the most preponderant. Indeed gadolinium is an extracellular CA (prevalent interstitial space distribution), thus it does not accumulate in the normal myocardium since the tissue volume is predominantly intracellular. Acute myocardial necrosis causes an increase in distribution volume due to membrane rupture, resulting in an expanded extracellular volume which translates into a high gadolinium concentration, thus shortened T1 relaxation and hyperenhancement. However, it has to be kept in mind that Gd-based CAs are neither necrotic nor fibrotic specific, and thus their concentration per voxel (volumetric unit of images) is influenced by any conditions altering extracellular volume (e.g., myocardial edema). In a pioneering study Reimer *et al.* demonstrated that 2-4 days after reperfusion in the infarcted myocardium there is a 25% increase in water content in conjunction with inflammation and hemorrhage (21). Accordingly, LGE technique may overestimate myocardial necrosis in the very early phase when the volume of the infarcted tissue tends to increase due phenomena other than myocytes necrosis, such as hyperemia, edema and inflammation cells infiltration. Recent studies showed a significant decrease in extent of enhancement between day 1 and day 7 post-infarction, suggesting an overestimation of the extent of irreversible damage at very early imaging (day 1) (22). These findings have to be considered when performing LGE technique for necrosis quantification in the early post-infarction phase. However, the extent of LGE early after an acute MI is strongly and independently associated with adverse ventricular remodeling and worse patient outcome (23). Also in patients with healed or unrecognized myocardial infarctions, the presence and extent of ischemic scar on contrast-enhanced MRI shows strong, and independent association with major adverse cardiovascular event and cardiac mortality (24,25).

Thanks to the high spatial resolution of LGE technique and the elevated difference in signal intensity between normal and necrotic myocardium, MI can be visualized with excellent accuracy and reproducibility outperforming other imaging modalities like SPECT imaging (26,27). It follows that LGE imaging allows a precise and reproducible quantification of irreversible damaged myocardium in term of infarct transmural (subendocardial vs. transmural) and mass (grams of necrosis/fibrosis). Infarct transmural can be expressed using a semi-quantitative score, for example dividing the myocardial wall in 4 equidistant segments (26), or using an automated quantification approach (28). In addition, infarction involving small but functionally important cardiac

structures, such as papillary muscles or right ventricular (RV) wall, can be easily identified. The current established techniques for RV infarct detection underestimate the true incidence of RV ischemic injury (29). In a recent study, we observed RV edema and LGE in as many as 75% and 54%, respectively, of patients with acute inferior LV infarction (30) (*Figure 4*). Interestingly, RV wall edema and LGE was observed in 33% and 11%, respectively, of patients with an acute anterior LV infarction. This is due to the fact that a considerable portion of anterolateral RV free wall is perfused by small branches of LAD coronary artery. The persistence of LGE of RV wall at 4 months after MI was associated with the absence of regional and global RV function recovery. The ability of LGE imaging to depict myocardial necrosis as small as 1 gram renders this technique ideal for depicting post PCI infarction. Two types of LGE patterns due to PCI-related myocardial necrosis have been described, i.e. "adjacent" myonecrosis in the neighborhood of the stent related to side-branch occlusion, and "distal" myonecrosis due to distal embolization of plaque material (31).

In reperfused acute MI, contrast-enhanced MRI, additionally enables to accurately identify the occurrence of MVO. Indeed, it is important to keep in mind that although primary PCI is effective to achieve an early and sustained patency of the infarct-related artery, a considerable proportion of ST-segment elevation MI patients (ranging between 5% and 50% according to the modalities) shows impaired myocardial reperfusion due to coronary microvascular dysfunction (32). Microvascular obstruction has a complex and multifactorial pathogenesis including: distal embolization, ischemia-reperfusion injury, compression due to myocardial cell swelling and interstitial edema, microvessel plugging by neutrophils and platelets, and dislodgment of microemboli from the epicardial coronary thrombus (32,33). On contrast-enhanced imaging, MVO typically appears as a subendocardially located hypointense area within the hyperenhanced myocardium (i.e. infarcted myocardium), and is clearly distinguishable from completely reperfused infarcts which present as homogeneous hyperenhanced myocardium. Judd *et al.* (34) validated the post-contrast cardiac MRI findings of no-reflow using thioflavin-S to demarcate no-reflow regions (*Figure 2,3*). In 52 reperfused ST-elevation MI's, we found a reduction in number (32 versus 27 of patients) and spatial extent of no-reflow ($36 \pm 25\%$ versus $16 \pm 14\%$ of late enhancement extent) between early and late contrast-enhanced MRI (35). Currently, first-pass perfusion imaging or contrast-enhanced MRI are used for MVO imaging (36). However, the former may be not ideal to

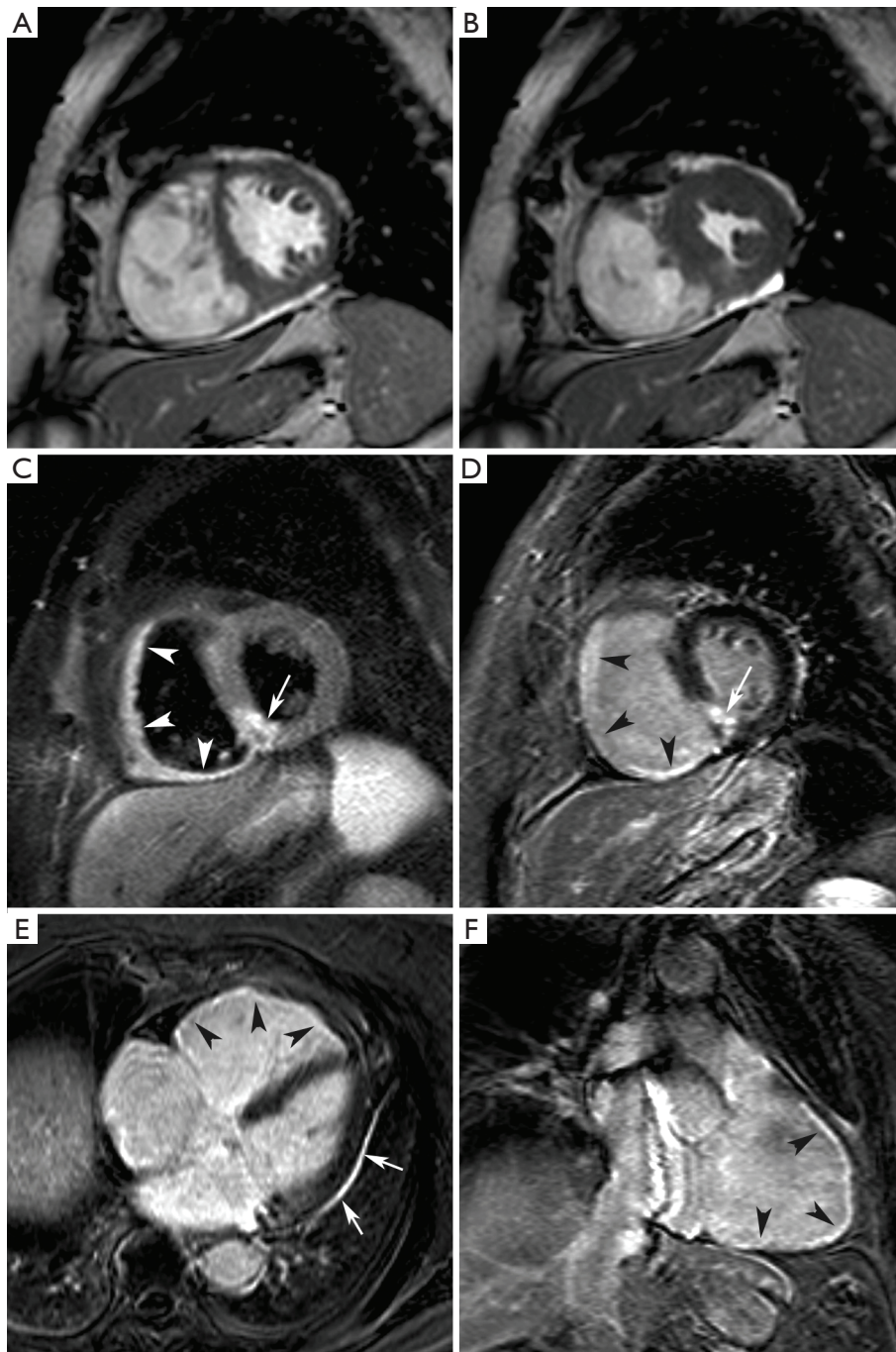


Figure 4 Nearly isolated RV infarction in 82-year-old woman. Short-axis cine at end diastole (A) and end systole (B), short-axis T2 weighted STIR imaging (C). Late gadolinium imaging in short-axis (D), horizontal long-axis (E) and RV vertical long-axis (F). Moderately dilated and dysfunctional RV (EDV: 197 mL, EF: 39%) and nearly normal LV volumes and function (EDV: 109 mL, EF: 63%). Diffuse RV myocardial edema (*arrowheads*, C) with limited edema in inferoseptal LV wall (*arrow*, C). Late gadolinium imaging shows diffuse RV myocardial enhancement (*arrowheads*, D,E,F). Focal transmural enhancement in inferoseptal LV wall (*arrow*, D). Note the presence of some pericardial enhancement along the lateral LV border (*arrows*, E). Adapted from Ischemic Heart Disease by Bogaert J and Dymarkowski S, in *Clinical Cardiac MRI Second Edition*, Bogaert J, Dymarkowski S, Taylor AM, Muthurangu V (eds). Springer Heidelberg, Germany (ISBN 978-3-642-23034-9)

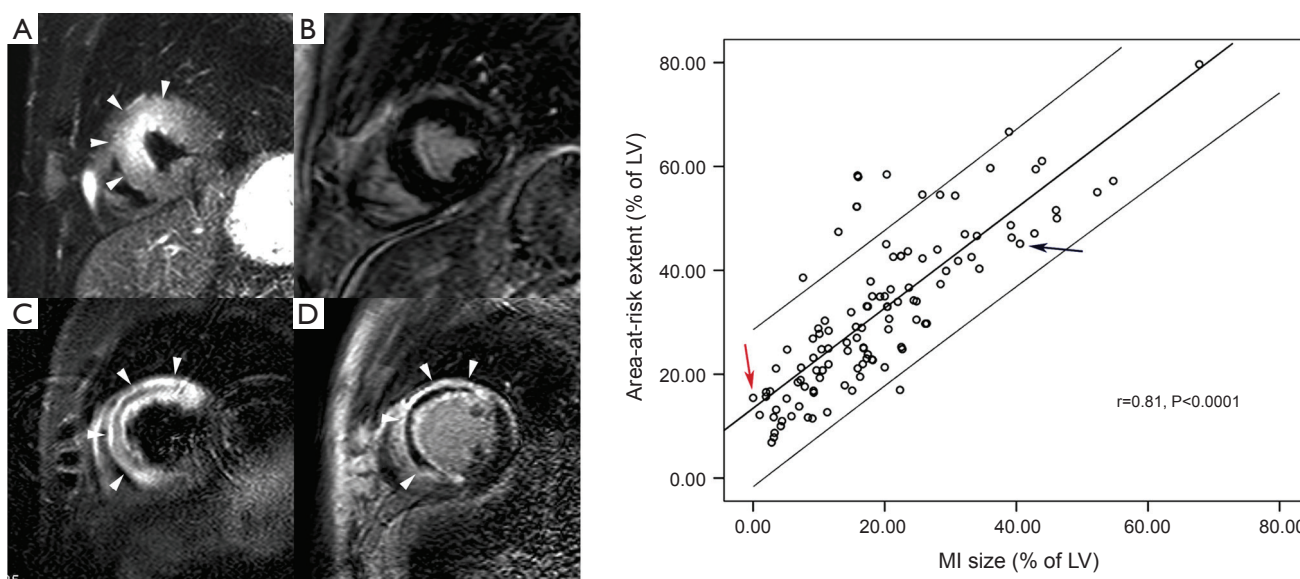


Figure 5 Complementary value of T2-weighted STIR imaging (A,C) and late gadolinium imaging (B,D) in acute infarct imaging. A first patient shows a large area of myocardial edema in the anteroseptal LV wall (*arrowheads*, A) but not late enhancement (B), corresponding to an aborted infarction. The second patient equally shows an extensive area of myocardial edema in the anteroseptal LV wall (*arrowheads*, C). Following contrast administration, strong enhancement occurs in the anteroseptal LV wall (*arrowheads*, D). The extent of enhancement nearly equals the extent of myocardial edema, leaving no or at most a minimal amount of myocardial salvage. In addition, this patient shows a large central hypo-intense zone within the edematous myocardium corresponding to myocardial hemorrhage (C), and an extensive area of microvascular obstruction (D). The relationship between extent of myocardial edema (i.e. area-at-risk) and extent of late enhancement (i.e. MI size), obtained in 137 patients, is shown in the graph (adapted from Masci *et al.* 2010). On the graph, patient one is shown by the red arrow, patient two by the blue arrow

evaluate the extent of no-reflow because of the limited number of image slices, the lower spatial resolution and the dynamic nature of first-pass. As an appealing alternative, early contrast-enhanced MRI (1-4 minutes) can be recommended since it allows full coverage of the left ventricle with better spatial resolution images (*Figure 2*) (35). While several groups use early post-contrast imaging for no-reflow imaging, others reported that late hypo-enhancement core visualized on LGE imaging was the best prognostic marker of LV remodeling (37,38). It is likely that at the time of late imaging, infarcts with small no-reflow zones have become homogeneously enhanced by wash-in of contrast in the low/no reflow areas, so that only the infarcts with severe microvascular damage were considered as true no-reflow infarcts. Because of this discrepancy regarding timing further research is required to define the optimal time point for no-reflow imaging. No reflow is related to more severe myocardial damage, increases with the duration of ischemia time and is independently associated with lack of functional recovery, adverse ventricular remodeling and worse patient outcome (39-42). In a study by Rochitte *et al.* using contrast enhanced MRI a 3-fold increase in the central

hypo-enhanced region was found during the first 48 hours after reperfusion, suggestive of progressive microvascular damage after reperfusion (43). These results are consistent with progressive microvascular and myocardial injury after reperfusion (41). Since MVO is composed of several degrees of severity, the microvascular damage is most severe in the infarct core, causing a complete occlusion (no-reflow), while in the peripheral layers less severe damage causing sub-obstruction presents as low-reflow (44). This might explain the observed differences in spatial extent between myocardial contrast echocardiography and contrast-enhanced MRI (41). Thus in patients with acute MI a comprehensive cardiac MRI study performed in the first week after the acute event allows to obtain an accurate estimate of myocardium at risk, microvascular damage and extent of infarction (*Figure 2*).

Additionally, myocardial salvage can be derived by subtracting the infarct size from the amount of myocardium at risk (*Figure 5*). Myocardial salvage is independently associated with early ST-segment resolution (45), and is an independent predictor of adverse LV remodeling and major cardiac events (ie, cardiac deaths, nonfatal myocardial infarction) at intermediate follow-up (45,46). Although

the myocardium at risk exceeds the irreversible damaged myocardium, but both are closely related (45). Interestingly in a cardiac MRI study by Francone *et al.* (47), it was shown that increasing ischemia time does not affect extent of myocardium at risk but results in an increasing infarct size and subsequently decreased myocardial salvage. In particular salvaged myocardium was markedly reduced after 90 min of coronary occlusion. Early mechanical reperfusion and maintenance of antegrade or collateral flow independently preserves myocardial salvage primarily through a reduction of infarct transmural. Myocardial salvage corrects the extent of MI by area at risk rendering this index particularly attractive as a surrogate end-point for testing novel or adjunctive reperfusion strategies.

Characterization of chronic myocardial infarction, post-infarction remodeling and myocardial viability

Immediately after an acute MI a series of pathophysiological changes take place in the necrotic myocardium aiming at replacing the death tissue with a firm fibrotic scar, whereas the non-infarcted myocardium compensates the loss of function of the infarcted myocardium in order to maintain an adequate cardiac output. Autopsy studies indicate that in humans the replacement of necrotic myocardium with a firm fibrotic scar may take up to 6 weeks, and it may be potentially influenced by the reperfusion status (1). The progressive substitution of the necrotic myocardium with the scar is associated with shrinkage of the damaged area, a phenomenon devoted to minimize the amount of dysfunctional myocardium and opposing to the expansion of the infarcted wall. Cardiac MRI studies indicate that LGE volumes reduces consistently between the acute and mid-term follow-up after MI. Ganame *et al.* (48) studied patients with acute ST-segment elevation MI undergoing primary PCI using cardiac MRI at early, 4 months and 1 year post-infarction. The authors demonstrated that there was a reduction of LGE mass of about 40% between early and 4 months post-infarction phase, whereas no further significant reduction was found at 1 year. It is therefore conceivable that most infarct healing occurs during the 4 months after the acute event (*Figure 3*). In this time course also the peri-infarcted myocardium (adjacent) became thinner and dysfunctional likely due to direct tethering of the neighboring necrotic/fibrotic myocardium. However, LV remodeling continues up to 1 year after the acute event, characterized by non-infarct remote wall thinning, at least in part related to augmented end-diastolic wall stress, increasing

LV volumes and evolution towards a more spherical LV configuration (*Figure 6*). These findings contradict the so far accepted concept that the remote non-infarcted myocardium develops compensatory hypertrophy in the post-infarction period (49-52), and warrant further investigation. Recently, we also addressed whether the relationship between infarct location and size and their reciprocal influences on post-infarction remodeling (53). In three tertiary centers, we studied by cardiac MRI 260 patients with acute ST-segment elevation MI undergoing primary PCI at early and 4 months post-infarction. We observed that patients with anterior MI experienced more pronounced post-infarction LV remodeling and dysfunction than those with inferior or lateral MIs because of the larger burden of necrosis without any independent contribution of infarct location *per se*. Using myocardial tagging cardiac MRI, a highly sensitive method measuring myocardial deformation, Bogaert *et al.* (54) also reported that dysfunction of non-infarcted remote myocardium occurred also at very early post-infarction phase contributing significant to overall LV remodeling and dysfunction. This was likely the consequence of the changes occurring in the infarct region leading to increased longitudinal wall stress rather than to loss of intrinsic contractility. In another study, using tagging and LGE cardiac MRI Bogaert *et al.* (55) studied patients with transmural anterior MI at 1 week and 3 months after the acute event. Tagging cardiac MRI was used to regionally quantify the deformation of the small rim of viable epicardium in the infarcted wall. They observed that sub-epicardial fiber shortening improved during follow-up and this was associated with increased regional ejection-fraction opposing to infarct expansion with favorable repercussions on overall LV remodeling and function recovery. Thus, the healing pattern of the infarcted myocardium influences not only remodeling and residual function of the infarcted region, but also the adaptive response of peri-infarcted (adjacent) and remote myocardium with important consequences on the overall geometry and function of the left ventricle. It is noteworthy that the magnitude of infarct shrinkage is highly anisotropic being different in radial, circumferential and longitudinal directions. Fieno *et al.* (52) studied serially the time course and geometry changes in infarcted and non-infarcted regions in a canine model of reperfused infarction. The authors showed that radial infarct thickness decreased progressively whereas changes in circumferential and longitudinal directions were variable. The preferential infarct resorption along the radial direction is associated with progressive thinning of the infarct wall, even though a certain degree

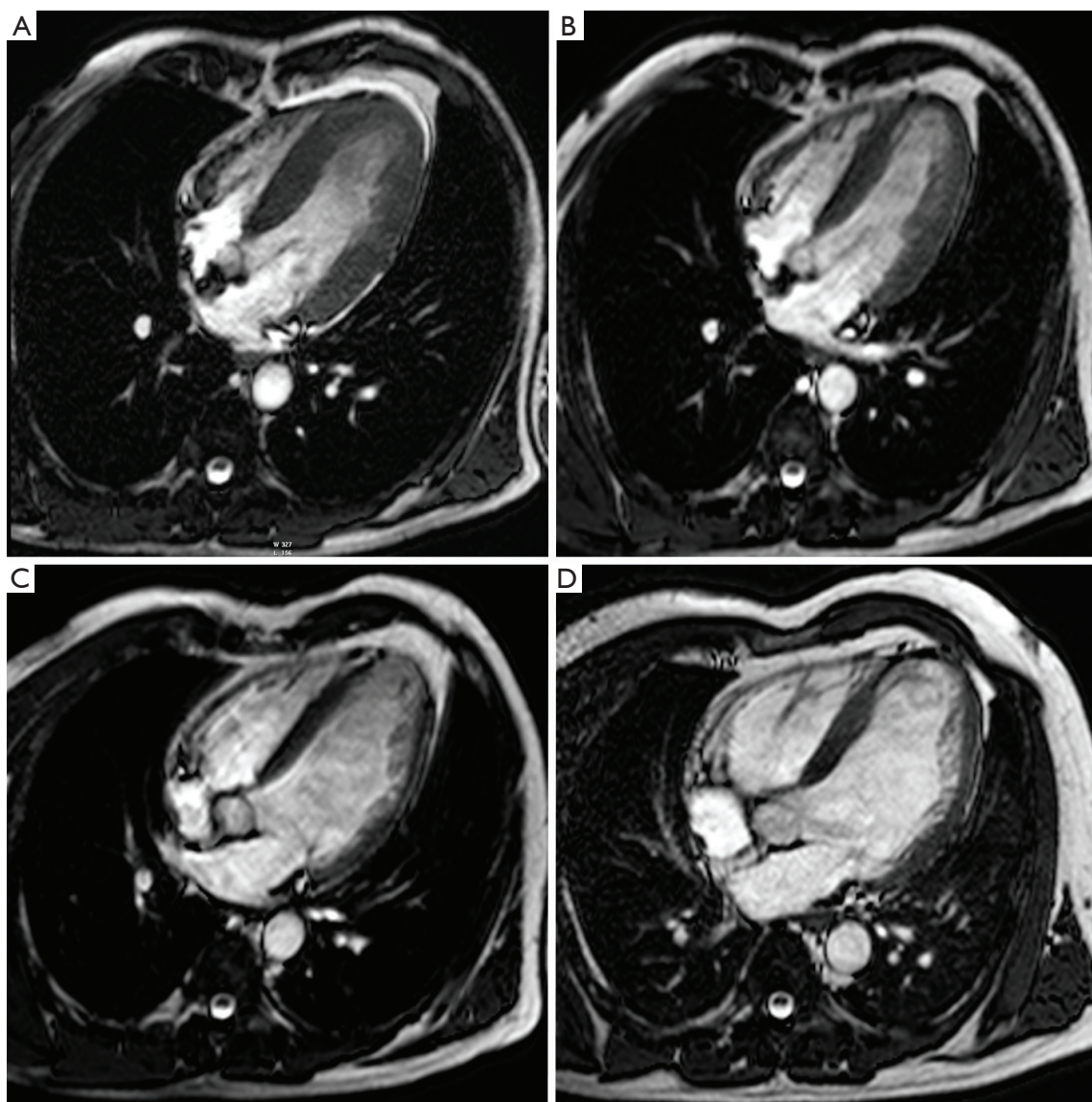


Figure 6 Use of MRI for long-term follow-up of ventricular remodeling post myocardial infarction in a patient with an extensive anteroapical MI. Horizontal long-axis cine imaging at 1 week (A), 4 months (B), 1 year (C), and 5 years (D) after the acute event (end-diastolic time frames). Cine imaging allows to appreciate the infarct healing with thinning of the LV apex, and the progressive LV dilatation over time (A-D). The LV end-diastolic volumes at 1 week, 4 months, 1 year and 5 years are 167 mL, 180 mL, 230 mL, 257 mL respectively. Adapted from *Ischemic Heart Disease* by Bogaert J and Dymarkowski S, in *Clinical Cardiac MRI Second Edition*, Bogaert J, Dymarkowski S, Taylor AM, Muthurangu V (eds). Springer Heidelberg, Germany (ISBN 978-3-642-23034-9)

of hypertrophy of viable epicardium may occur opposing to infarct wall thinning and favoring functional recovery. Experimentally, it has also been demonstrated that collagen fibers disposition parallels that of necrotic myocardial fibers mirroring the anisotropic structure of myocardium (56,57). This phenomenon aims at preserving the structural integrity of the infarcted wall resulting in the deposition of a resistant

but at same time elastic scar opposing to infarct expansion but at the same facilitating the recovery of function of the peri-infarcted (adjacent) myocardium. Experimentally, it has been demonstrated that scar anisotropy allows the scar to resist circumferential stretching while deforming compatibly with adjacent non-infarcted myocardium in the longitudinal and radial directions (30,31). Exploiting the high spatial

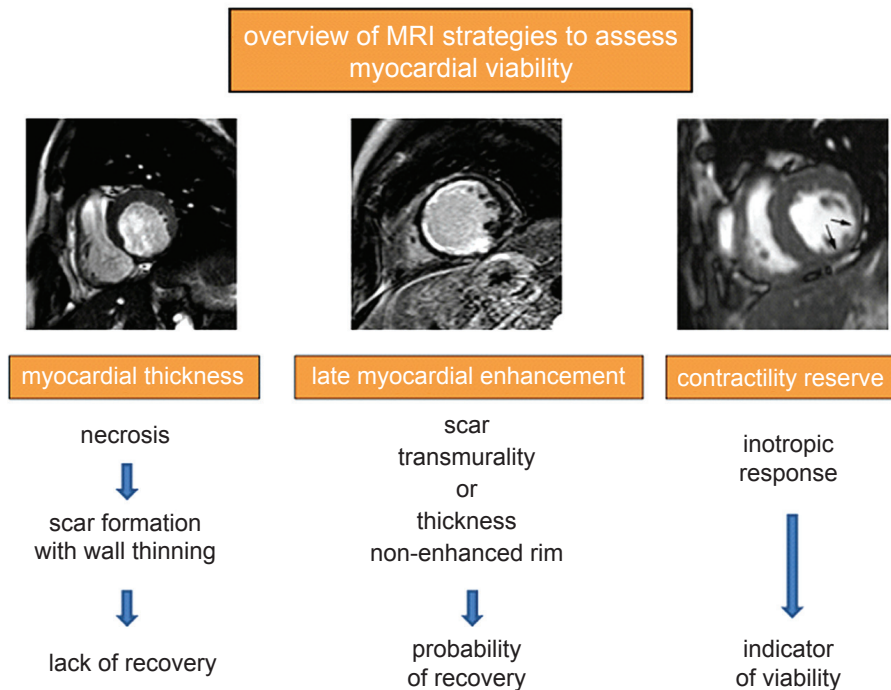


Figure 7 Overview of MRI strategies currently used to assess myocardial viability in patients presenting symptoms of chronic myocardial ischemia and LV dysfunction. Adapted from *Ischemic Heart Disease* by Bogaert J and Dymarkowski S, in *Clinical Cardiac MRI Second Edition*, Bogaert J, Dymarkowski S, Taylor AM, Muthurangu V (eds). Springer Heidelberg, Germany (ISBN 978-3-642-23034-9)

resolution, high contrast-to-noise ratio and non-invasive nature of the technique, serial comprehensive cardiac MRI studies can depict the complex remodeling processes occurring in the infarcted and non-infarcted myocardium and their relative influence on LV dilatation and dysfunction, offering a peculiar perspective in post-infarction remodeling.

Assessment of myocardial viability

Transient sub-lethal ischemia rapidly impairs contractile function, and this dysfunction can persist for hours after the restoration of normal blood flow. This phenomenon is known as myocardial stunning, and repeated episodes of transient ischemia may result in cumulative stunning contributing to chronic post-ischemic LV dysfunction (58). A severe reduction of coronary flow reserve is observed both in stunning and hibernation, and the functional recovery of hibernated myocardium is associated with restoration of an adequate flow reserve. It is important to emphasize that most of our knowledge on the clinical utility of pre-operative assessment of myocardial viability in patients with chronic LV post-ischemic dysfunction is based on retrospective studies. These indicate that viability test adds information

on in-hospital or 1-year prognosis when added to clinical and angiographic data. However, recently a sub-study of the STICH trial questioned the value of myocardial viability assessment in patients with ischemic cardiomyopathy (59). Indeed, the detection of myocardial viability by SPECT did not identify patients with a different survival benefit from bypass as compared to guidelines-based medical therapy. It is important to underline that, however, the study was neither designed nor powered to investigate the clinical utility of myocardial viability assessment by cardiac imaging resulting in selection and referral bias. The different approaches to assess myocardial viability and a timeline for a comprehensive exam are shown in *Figure 7*. Dobutamine-stress cardiac MRI at low-dose of dobutamine (5 to $10 \mu\text{g} \cdot \text{kg} \cdot \text{min}^{-1}$) increases contractility in dysfunctional but viable segments whereas at higher doses (up to $40 \mu\text{g} \cdot \text{kg} \cdot \text{min}^{-1}$ plus atropine) contractility may decrease reflecting inducible myocardial ischemia (60,61). The so called “biphasic response” is highly predictive of post-operative functional recovery (62). Left ventricular segments with transmural scar usually do not show functional recovery in contrast to those without significant scarring. Dobutamine stress MRI has a good specificity (83%, range 70-95%) but moderate sensitivity (74%, range

50-89%), values that are in line with those of dobutamine echocardiography (63). Contrast-enhanced cardiac MRI enables to accurately detect replacement myocardial fibrosis due to a previous MI. This is due to the fact that in fibrotic scars, similarly to what happens in acutely necrotic myocardium, the intracellular space is markedly reduced in favor of extracellular space yielding an accumulation of Gd-based CA in the scarred myocardium (64). As a result, on post-contrast LGE imaging the scarred myocardium appears hyperintense whereas the signal of normal myocardium is 'nulled' and appears black. In patients with stable IHD myocardial LGE frequently occurs in dysfunctional segments and is associated with nonviability obtained by SPECT imaging and dobutamine echocardiography, whereas absence of LGE correlates with measures of viability irrespective of resting function (65). In particular the likelihood of improvement in regional contractility after revascularization is inversely related to the transmural extent of hyperenhancement (66,67). In dysfunctional segments without hyperenhancement 78% improved contractility post-revascularization as compared to 2% of segments with scar tissue extending >75% of the LV wall (66). These findings resulted in a paradigm shift, i.e. the absence of LGE in a thinned (<5 mm) and dysfunctional myocardium, previously assumed to be non-viable myocardium, can potentially be associated with restoration of normal function after revascularization. Post-contrast LGE technique has an excellent sensitivity (97%, range 91-100%) but a relatively low specificity (68%, range 51-85%) (58). The relative low specificity can be ascribed to several factors: (I) short-term follow-up between revascularization and assessment of left ventricular function (time course of hibernating myocardium functional recovery can protract up to 14 months), (II) false positive results including those due to procedural injury, (III) incomplete revascularization, (IV) tethering of the adjacent scarring segments. Recently, Gerber *et al.* (68) studied 144 patients with chronic IHD and LV dysfunction by means of LGE cardiac MRI and they observed that over a 3 year median follow-up in those patients without revascularization the presence of dysfunctional but still viable myocardium identified by LGE technique was independent predictor of mortality. Recently concerns have been arisen about the safety on Gd-based CA in patients with severe renal failure due to a life-threatening condition known as nephrogenic systemic fibrosis (NSF). This entity is characterized by progressive and severe fibrosis of the skin, subcutaneous tissues and sometimes internal organs. Although it is a rare condition being associated with particularly high dosage of

Gd-based CA, the Food and Drug Administration and other regulatory committee recommend to use less or avoid Gd-based CA when estimated when the glomerular filtration rate (GFR) is estimated to be <30 mL/min. However a recent report examining 370 NSF cases showed that the risk can be consistently decrease by adopting by limiting GBCA dose to a maximum of 0.1 mmol/kg, dialyzing patients undergoing dialysis quickly following Gd-based CA administration, delaying Gd-based CA in acute renal failure until after renal function returns or dialysis is initiated, and avoiding nonionic linear Gd-based CA in patients with renal failure (69,70).

Conclusions

Cardiac MRI represents an appealing imaging technique for investigating acute and chronic IHD. In the acute phase, this modality allows to quantify and characterize the pattern of ischemic myocardial damage in term of area at risk and infarct size, and thereby of salvaged myocardium, along with the depiction of myocardial hemorrhage and microvascular obstruction. In the chronic IHD, cardiac MRI enables an accurate assessment of myocardial viability and inducible ischemia. Importantly these morphological information come along with the functional assessment consisting in an accurate quantification of LV volumes, regional and global systolic function. Thus, cardiac MRI allows an accurate and comprehensive insight into the pathophysiology of ischemic myocardial damage and the post-infarction remodeling. In the future the introduction of novel sequence for a quantitative assessment of T1 and T2 values of myocardium (T1 and T2 mapping, respectively) and hopefully the adoption of 'molecular' cardiac MRI approach also in humans will further expand our knowledge on IHD.

Acknowledgments

Disclosure: The authors declare no conflict of interest.

References

1. Fishbein MC, Maclean D, Maroko PR. The histopathologic evolution of myocardial infarction. *Chest* 1978;73:843-9.
2. Aletras AH, Tilak GS, Natanzon A, et al. Retrospective determination of the area at risk for reperfused acute myocardial infarction with T2-weighted cardiac magnetic resonance imaging. Histopathological and displacement encoding with stimulated echoes

- (DENSE) functional validations. *Circulation* 2006;113:1865-70.
3. Higgins CB, Herfkens R, Lipton MJ, et al. Nuclear magnetic resonance imaging of acute myocardial infarction in dogs: alterations in magnetic relaxation times. *Am J Cardiol* 1983;52:184-8.
 4. McNamara MT, Wesbey GE, Brasch RC. Magnetic resonance imaging of acute myocardial infarction using a nitroxyl spin label (PCA). *Invest Radiol* 1985;20:591-5.
 5. Cury RC, Shash K, Nagurney JT, et al. Cardiac magnetic resonance with T2-weighted imaging improves detection of patients with acute coronary syndrome in the emergency department. *Circulation* 2008;118:837-44.
 6. Raman SV, Simonetti OP, Winner MW III, et al. Cardiac magnetic resonance with edema imaging identifies myocardium at risk and predicts worse outcome in patients with non-ST-segment elevation acute coronary syndrome. *J Am Coll Cardiol* 2010;55:2480-8.
 7. Abdel-Aty H, Cocker M, Meek C, et al. Edema as a very early marker for acute myocardial ischemia: a cardiovascular magnetic resonance study. *J Am Coll Cardiol* 2009;53:1194-201.
 8. Carlson M, Ubachs JFA, Hedström E, et al. Myocardium at risk after acute infarction in humans on cardiac magnetic resonance. Quantitative assessment during follow-up and validation with single-photon emission computed tomography. *J Am Coll Cardiol Img* 2009;2:569-76.
 9. Ortiz-Pérez JT, Meyers SN, Lee DC, et al. Angiographic estimates of myocardium at risk during acute myocardial infarction: validation study using cardiac magnetic resonance Imaging. *Eur Heart J* 2007;28:1750-8.
 10. Wright J, Adriaenssens T, Dymarkowski S, et al. Quantification of myocardial area at risk with T2-weighted CMR: comparison with contrast-enhanced CMR and coronary angiography. *JACC Cardiovasc Imaging* 2009;2:825-31.
 11. Friedrich MG, Kim HW, Kim RJ. T2-weighted imaging to assess post-infarct myocardium at risk. *JACC Cardiovasc Imaging* 2011;4:1014-21.
 12. Giri S, Chung YC, Merchant A, et al. T2 quantification for improved detection of myocardial edema. *J Cardiovasc Magn Reson* 2009;11:56.
 13. Viallon M, Mewton N, Thuny F, et al. T2-weighted cardiac MR assessment of the myocardial area-at-risk and salvage area in acute reperfused myocardial infarction: comparison of state-of-the-art dark blood and bright blood T2-weighted sequences. *J Magn Reson Imaging* 2012;35:328-39.
 14. Abdel-Aty H, Zagrosek A, Schulz-Menger J, et al. Delayed enhanced and T2-weighted cardiovascular magnetic resonance imaging differentiate acute from chronic myocardial infarction. *Circulation* 2004;109:2411-6.
 15. Garcia-Dorado D, Théroux P, Solares J, et al. Determinants of hemorrhagic infarcts. Histologic observations from experiments involving coronary occlusion, coronary reperfusion, and reocclusion. *AJP* 1990;137:301-11.
 16. Basso C, Corbetti F, Silva C, et al. Morphologic validation of reperfused hemorrhagic myocardial infarction by cardiovascular magnetic resonance. *Am J Cardiol* 2007;100:1322-7.
 17. Lotan CS, Bouchard A, Cranney CB, et al. Pohost GM. Assessment of postreperfusion myocardial hemorrhage using proton NMR imaging at 1.5T. *Circulation* 1992;86:1018-25.
 18. Ganame J, Messalli G, Dymarkowski S, et al. Impact of myocardial hemorrhage on left ventricular function and remodelling in patients with reperfused acute myocardial infarction. *Eur Heart J* 2009;30:1440-9.
 19. Eitel I, Kubusch K, Strohm O, et al. Prognostic value and determinants of a hypointense infarct core in T2-weighted cardiac magnetic resonance in acute reperfused ST-elevation-myocardial infarction. *Circ Cardiovasc Imaging* 2011;4:354-62.
 20. Kim RJ, Fieno DS, Parrish TB, et al. Relationship of MRI delayed contrast enhancement to irreversible injury, infarct age, and contractile function. *Circulation* 1999;100:1992-2002.
 21. Reimer KA, Jennings RB. The changing anatomic reference base of evolving myocardial infarction. *Circulation* 1979;60:866-76.
 22. Engblom H, Hedström E, Heiberg E, et al. Rapid initial reduction of hyperenhanced myocardium after reperfused first myocardial infarction suggests recovery of the peri-infarction zone. One-year follow-up by MRI. *Circ Cardiovasc Imaging* 2009;2:47-55.
 23. Wu E, Ortiz JT, Tejedor P, et al. Infarct size by contrast enhanced cardiac magnetic resonance is a stronger predictor of outcomes than left ventricular ejection fraction or end-systolic volume index: prospective cohort study. *Heart* 2008;94:730-6.

24. Kwong RY, Chan AK, Brown KA, et al. Impact of unrecognized myocardial scar detected by cardiac magnetic resonance imaging on event-free survival in patients presenting with signs or symptoms or coronary artery disease. *Circulation* 2006;113:2733-43.
25. Roes SD, Kelle S, Kaandorp TA, et al. Comparison of myocardial infarct size assessed with contrast-enhanced magnetic resonance imaging and left ventricular function and volumes to predict mortality in patients with healed myocardial infarction. *Am J Cardiol* 2007;100:930-6.
26. Wagner A, Mahrholdt H, Holly TA, et al. Contrast-enhanced MRI and routine single photon emission computed tomography (SPECT) perfusion imaging for detection of subendocardial myocardial infarcts: an imaging study. *Lancet* 2003;361:374-9.
27. Ibrahim T, Bülow HP, Hackl T, et al. Diagnostic value of contrast-enhanced magnetic resonance imaging and single-photon emission computed tomography for detection of myocardial necrosis early after acute myocardial infarction. *J Am Coll Cardiol* 2007;49:208-16.
28. Berbari R, Kachenoura N, Frouin F, et al. An automated quantification of the transmural myocardial infarct extent using cardiac DE-MR images. *Conf Proc IEEE Eng Med Biol Soc* 2009;2009:4403-6.
29. Kumar A, Abdel-Aty H, Kriedemann I, et al. Contrast-enhanced cardiovascular magnetic resonance imaging of right ventricular infarction. *J Am Coll Cardiol* 2006;48:1969-76.
30. Masci PG, Francone M, Desmet W, et al. Right ventricular ischemic injury in patients with acute ST-segment elevation myocardial infarction. Characterization with cardiovascular magnetic resonance. *Circulation* 2010;122:1405-12.
31. Porto I, Selvanayagam JB, Van Gaal WJ, et al. Plaque volume and occurrence and location of periprocedural myocardial necrosis after percutaneous coronary intervention. Insights from delayed-enhancement magnetic resonance imaging, thrombolysis in myocardial infarction myocardial perfusion grade analysis, and intravascular ultrasound. *Circulation* 2006;114:662-9.
32. Wang X, Nie SP. The coronary slow flow phenomenon: Characteristics, mechanisms and implications. *Cardiovasc Diagn Ther* 2011;1:37-43.
33. Kloner RA, Ganote CE, Jennings RB. The 'no-reflow' phenomenon after temporary coronary occlusion in the dog. *J Clin Invest* 1974;54:1496-508.
34. Judd RM, Lugo-Olivieri CH, Arai M, et al. Physiological basis of myocardial contrast enhancement in fast magnetic resonance images of 2-day-old reperfused canine infarcts. *Circulation* 1995;92:1902-10.
35. Bogaert J, Kalantzi M, Rademakers FE, et al. Determinants and impact of microvascular obstruction in successfully reperfused ST-segment elevation myocardial infarction. Assessment by magnetic resonance imaging. *Eur Radiol* 2007;17:2572-80.
36. Taylor AJ, Al-Saadi N, Abdel-Aty H, et al. Detection of acutely impaired microvascular reperfusion after infarct angioplasty with magnetic resonance imaging. *Circulation* 2004;109:2080-5.
37. Nijveldt R, Beek AM, Hirsch A, et al. Functional recovery after acute myocardial infarction. Comparison between angiography, electrocardiography, and cardiovascular magnetic resonance measures of microvascular injury. *J Am Coll Cardiol* 2008;52:181-9.
38. Nijveldt R, Hofman MBM, Hirsch A, et al. Assessment of microvascular obstruction and prediction of short-term remodeling after acute myocardial infarction: cardiac MR imaging study. *Radiology* 2009;250:363-70.
39. Rogers WJ, Kramer CM, Geskin G, et al. Early contrast-enhanced MRI predicts late functional recovery after reperfused myocardial infarction. *Circulation* 1999;99:744-50.
40. Wu KC, Zerhouni EA, Judd RM, et al. Prognostic significance of microvascular obstruction by magnetic resonance imaging in patients with acute myocardial infarction. *Circulation* 1998;97:765-72.
41. Wu KC, Kim RK, Bluemke DA, et al. Quantification and time course of microvascular obstruction by contrast-enhanced echocardiography and magnetic resonance imaging following acute myocardial infarction and reperfusion. *J Am Coll Cardiol* 1998;32:1756-64.
42. Hombach V, Grebe O, Merkle N, et al. Sequelae of acute myocardial infarction regarding cardiac structure and function and their prognostic significance as assessed by magnetic resonance imaging. *Eur Heart J* 2005;26:549-57.
43. Rochitte CE, Lima JA, Bluemke DA, et al. Magnitude and time course of microvascular obstruction and tissue injury after acute myocardial infarction. *Circulation* 1998;98:1006-14.
44. Reimer KA, Jennings RB. The wavefront progression of myocardial ischemic cell death. II. Transmural progression of necrosis within the framework of

- ischemic bed size (myocardium at risk) and collateral flow. *Lab Invest* 1979;40:633-44.
45. Masci PG, Ganame J, Strata E, et al. Myocardial salvage by CMR correlates with LV remodeling and early ST-segment resolution in acute myocardial infarction. *JACC Cardiovasc Imaging* 2010;3:45-51.
 46. Eitel I, Desch S, Fuernau G, et al. Prognostic significance and determinants of myocardial salvage assessed by cardiovascular magnetic resonance in acute reperfused myocardial infarction. *J Am Coll Cardiol* 2010;55:2470-9.
 47. Francone M, Bucciarelli-Ducci C, Carbone I, et al. Impact of primary coronary angioplasty delay on myocardial salvage, infarct size, and microvascular damage in patients with ST-segment elevation myocardial infarction. Insight from cardiovascular magnetic resonance. *J Am Coll Cardiol* 2009;54:2145-53.
 48. Ganame J, Messalli G, Masci PG, et al. Time course of infarct healing and left ventricular remodeling in patients with reperfused ST-segment elevation myocardial infarction using comprehensive magnetic resonance imaging. *Eur Radiol* 2011;21:693-701.
 49. Holmes JW, Yamashita H, Waldman LK, et al. Scar remodeling and transmural deformation after infarction in the pig. *Circulation* 1994;90:411-20.
 50. Mitchell GF, Lamas GA, Vaughan DE, et al. Left ventricular remodeling in the year after first anterior myocardial infarction: a quantitative analysis of contractile segment lengths and ventricular shape. *J Am Coll Cardiol* 1992;19:1136-44.
 51. McKay RG, Pfeffer MA, Pasternak RC, et al. Left ventricular remodeling after myocardial infarction: a corollary to infarct expansion. *Circulation* 1986;74:693-702.
 52. Fieno DS, Hillenbrand HB, Rehwald WG, et al. Infarct resorption, compensatory hypertrophy, and differing patterns of ventricular remodeling following myocardial infarctions of varying size. *J Am Coll Cardiol* 2004;43:2124-31.
 53. Masci PG, Ganame J, Francone M, et al. Relationship between location and size of myocardial infarction and their reciprocal influences on post-infarction left ventricular remodeling. *Eur Heart J* 2011;32:1640-8.
 54. Bogaert J, Bosmans H, Maes A, et al. Remote myocardial dysfunction after acute anterior myocardial infarction: impact of left ventricular shape on regional function. A magnetic resonance myocardial tagging study. *J Am Coll Cardiol* 2000;35:1525-34.
 55. Bogaert J, Maes A, Van de Werf F, et al. Functional recovery of subepicardial myocardial tissue in transmural myocardial infarction after successful reperfusion. An important contribution to the improvement of regional and global left ventricular function. *Circulation* 1999;99:36-43.
 56. Holmes JW, Nuñez JA, Covell JW. Functional implications of myocardial scar structure. *Am J Physiol* 1997;272:H2123-30.
 57. Zimmerman SD, Karlon WJ, Holmes JW, et al. Structural and mechanical factors influencing infarct scar collagen organization. *Am J Physiol Heart Circ Physiol* 2000;278:H194-H200.
 58. Camici PG, Prasad SK, Rimoldi OE. Stunning, hibernation, and assessment of myocardial viability. *Circulation* 2008;117:103-14.
 59. Bonow RO, Maurer G, Lee KL, et al; STICH Trial Investigators. Myocardial viability and survival in ischemic left ventricular dysfunction. *N Engl J Med* 2011;364:1617-25.
 60. Dendale PAC, Franken RP, Waldmann GJ, et al. Low-dosage dobutamine magnetic resonance imaging as an alternative to echocardiography in the detection of viable myocardium after acute infarction. *Am Heart J* 1995;130:134-40.
 61. Dendale P, Franken PR, van der Wall EE, et al. Wall thickening at rest and contractile reserve early after myocardial infarction: correlation with myocardial perfusion and metabolism. *Coron Artery Dis* 1997;8:259-64.
 62. Senior R, Lahiri A. Enhanced detection of myocardial ischemia by stress dobutamine echocardiography utilizing the "biphasic" response of wall thickening during low and high dose dobutamine infusion. *J Am Coll Cardiol* 1995;26:26-32.
 63. Kaandorp TAM, Lamb HJ, van der Wall EE, et al. Cardiovascular MR to assess myocardial viability in chronic ischaemic LV dysfunction. *Heart* 2005;91:1359-65.
 64. Rehwald WG, Fieno DS, Chen EL, et al. Myocardial magnetic resonance imaging contrast agent concentrations after reversible and irreversible ischemic injury. *Circulation* 2002;105:224-9.
 65. Ramani K, Judd RM, Holly TA, et al. Contrast magnetic resonance imaging in the assessment of myocardial viability in patients with stable coronary artery disease and left ventricular dysfunction. *Circulation* 1998;98:2687-94.
 66. Kim RJ, Wu E, Rafael A, et al. The use of contrast-enhanced magnetic resonance imaging to identify

- reversible myocardial dysfunction. *N Engl J Med* 2000;343:1445-53.
67. Selvanayagam JB, Kardos A, Francis JM, et al. Value of delayed-enhancement cardiovascular magnetic resonance imaging in predicting myocardial viability after surgical revascularization. *Circulation* 2004;110:1535-41.
68. Gerber BL, Rousseau MF, Ahn SA, et al. Prognostic value of myocardial viability by delayed-enhanced magnetic resonance in patients with coronary artery disease and low ejection fraction: impact of revascularization therapy. *J Am Coll Cardiol* 2012;59:825-35.
69. Leiner T, Kucharczyk W. NSF prevention in clinical practice: summary of recommendations and guidelines in the United States, Canada, and Europe. *J Magn Reson Imaging* 2009;30:1357-63.
70. Zou Z, Zhang HI, Roditi GH, et al. Nephrogenic Systemic Fibrosis. Review of 370 Biopsy-Confirmed Cases. *JACC Cardiovasc Imaging* 2011;4:1206-16.

Cite this article as: Masci PG, Bogaert J. Post myocardial infarction of the left ventricle: the course ahead seen by cardiac MRI. *Cardiovasc Diagn Ther* 2012;2(2):113-127. doi: 10.3978/j.issn.2223-3652.2012.04.06